γδTCR recruits the Syk/PI3K axis to drive proinflammatory differentiation program

Ryunosuke Muro,[1,2] Takeshi Nitta,[2] Kenta Nakano,[3] Tadashi Okamura,[3,4] Hiroshi Takayanagi,[2] and Harumi Suzuki[1]

[1]Department of Immunology and Pathology, Research Institute, National Center for Global Health and Medicine, Chiba, Japan. [2]Department of Immunology, Graduate School of Medicine and Faculty of Medicine, The University of Tokyo, Tokyo, Japan. [3]Department of Laboratory Animal Medicine, and [4]Section of Animal Models, Research Institute, National Center for Global Health and Medicine, Tokyo, Japan.

γδT cells produce inflammatory cytokines and have been implicated in the pathogenesis of cancer, infectious diseases, and autoimmunity. The T cell receptor (TCR) signal transduction that specifically regulates the development of IL-17–producing γδT (γδT17) cells largely remains unclear. Here, we showed that the receptor proximal tyrosine kinase Syk is essential for γδTCR signal transduction and development of γδT17 in the mouse thymus. Zap70, another tyrosine kinase essential for the development of αβT cells, failed to functionally substitute for Syk in the development of γδT17. Syk induced the activation of the PI3K/Akt pathway upon γδTCR stimulation. Mice deficient in PI3K signaling exhibited a complete loss of γδT17, without impaired development of IFN-γ–producing γδT cells. Moreover, γδT17-dependent skin inflammation was ameliorated in mice deficient in RhoH, an adaptor known to recruit Syk. Thus, we deciphered lineage-specific TCR signaling and identified the Syk/PI3K pathway as a critical determinant of proinflammatory γδT cell differentiation.

Introduction

γδT cells have recently attracted considerable attention because of their inflammatory cytokine–producing potential and their contribution to various pathophysiological states. A subset of γδT cells that produces IL-17 (termed γδT17 cells) plays a pivotal role not only in protection against bacterial and fungal infection (1) but also in the progression of inflammatory disorders (2–4), tumor growth and metastasis (5–8), and tissue regeneration (9). The cytokine-producing potential of γδT cells is programmed during their development in the thymus (10, 11).

Unlike αβT cells, the development of which is dependent on positive and negative selections upon the interaction between αβ T cell receptor (αβTCR) and peptide-MHC complexes, γδT cells do not require γδTCR recognition of ligands for their development in the thymus. Self-oligomerization of γδTCR at the cell surface of precursor thymocytes induces their differentiation into mature γδT cells (12, 13). It has been proposed that γδTCR-ligand interaction determines the effector function of γδT cells (14). γδT cells that receive the ligand-dependent strong or ligand-independent weak γδTCR signals are induced to differentiate into IFN-γ–producing or IL-17–producing subsets, respectively (12, 15). However, the molecular basis for this remains unclear.

Rearranged TCR chains (α/β or γ/δ), together with CD3 subunits (γ, δ, ε, and ζ), form TCR-CD3 complexes, which initiate the sequential phosphorylation of proximal tyrosine kinases and activation of downstream signaling pathways in response to ligand-dependent or ligand-independent oligomerization (16). A series of studies have indicated the differences between αβT and γδT cells in terms of the TCR-CD3 complex structure and downstream signals. Although the CD3δ subunit is contained in αβTCR, it is barely detectable in γδTCR complexes (17). CD3δ subunit–deficient mice exhibit a developmental arrest of αβT cells but not γδT cells (18). The mutation of CD3ε (C80G) that prevents conformational changes in TCR-CD3 complexes completely inhibits αβT cell development at an early stage. However, it does not impair the development of certain γδT cell subsets (19). A recent report showed that mice haploinsufficient for CD3γ and CD3δ (*CD3g*$^{+/-}$ *CD3d*$^{+/-}$) have reduced TCR signaling and abnormal differentiation in γδT cells but not αβT cells (20). αβT and γδT cells also show differential requirements of the Src family kinases in their development. In Lck/Fyn–doubly deficient mice, αβT cell development is completely inhibited, whereas γδT cell development is partially impaired (21, 22). Moreover, γδT cells require Blk, an Src family kinase primarily expressed in B cells, for the induction of the γδT17 subset (23). These findings indicate that the TCR-CD3 complexes and TCR proximal signaling modules in γδT cells are distinct from those in αβT cells.

In the present study, we investigated the molecular mechanism underlying γδTCR signaling that determines the development and effector function of γδT cells. We found that Syk, a tyrosine kinase known to associate with the B cell receptor (BCR) and Fc receptor, was pivotal for γδTCR signal transduction and γδT17 development. Our present results revealed that the deficiency of Syk, but not Zap70, completely abolished the development of γδT17 and that Zap70 failed to functionally substitute Syk in γδT17 development. We also showed that Syk distinctively induced the development of γδT17 through activation of the PI3K/Akt pathway. These results provide a mechanistic insight into the Syk-mediated TCR signal transduction in the determination of γδT cell fate.

Results

Preferential requirement of Syk rather than Zap70 in γδTCR signals and γδT cell development. To characterize the intracellular signal

Authorship note: R. Muro and T. Nitta are co–first authors.
Conflict of interest: The authors have declared that no conflict of interest exists.
Submitted: June 21, 2017; **Accepted:** October 31, 2017.
Reference information: *J Clin Invest*. 2018;128(1):415–426.
https://doi.org/10.1172/JCI95837.

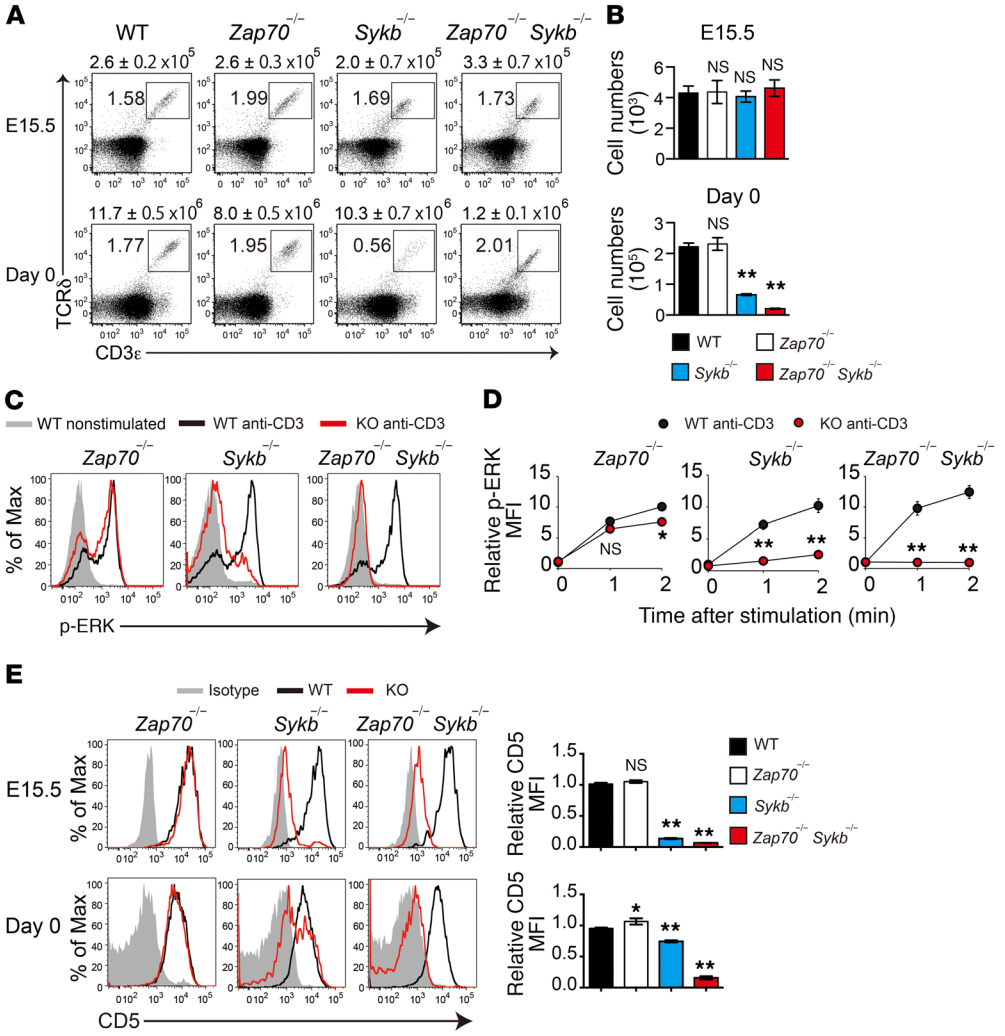

Figure 1. Syk plays a dominant role in γδTCR signaling and γδT cell development. (**A** and **B**) Flow cytometric analysis of CD3ε and TCRδ expression in thymocytes from the indicated mice at E15.5 (WT, $n = 16$; *Zap70*$^{-/-}$, $n = 10$; *Sykb*$^{-/-}$, $n = 8$; and *Zap70*$^{-/-}$ *Sykb*$^{-/-}$, $n = 2$) and on day 0 (WT, $n = 19$; *Zap70*$^{-/-}$, $n = 4$; *Sykb*$^{-/-}$, $n = 7$; and *Zap70*$^{-/-}$ *Sykb*$^{-/-}$, $n = 8$). The total number of thymocytes is indicated above each flow cytometric plot (**A**). Graphs indicate the total number of γδT cells per mouse (**B**). (**C** and **D**) TCR-induced ERK phosphorylation in thymic γδT cells from the indicated mice on day 0 (*Zap70*$^{-/-}$, $n = 3$; *Sykb*$^{-/-}$, $n = 4$; and *Zap70*$^{-/-}$ *Sykb*$^{-/-}$, $n = 3$). Histograms indicate p-ERK levels after a 2-minute stimulation (**C**). MFI relative to the nonstimulated control (**D**). (**E**) Histograms show CD5 expression in thymic γδT cells from the indicated mice at E15.5 (WT, $n = 13$; *Zap70*$^{-/-}$, $n = 10$; *Sykb*$^{-/-}$, $n = 9$; and *Zap70*$^{-/-}$ *Sykb*$^{-/-}$, $n = 2$) and on day 0 (WT, $n = 17$; *Zap70*$^{-/-}$, $n = 3$; *Sykb*$^{-/-}$, $n = 7$; and *Zap70*$^{-/-}$ *Sykb*$^{-/-}$, $n = 5$). Graphs indicate the MFI relative to WT mice. All data represent the mean ± SEM. $^*P < 0.05$ and $^{**}P < 0.01$, by 1-way ANOVA (**B** and **E**) and 2-way ANOVA (**D**). Data represent the combined results of 3 independent experiments (**A**, **B**, and **E**) or a single experiment (**C** and **D**). Max, maximum.

transduction downstream of γδTCR, we examined protein tyrosine phosphorylation in ex vivo γδT cells isolated from the mouse thymus. In response to γδTCR engagement with anti-CD3ε antibody, we detected tyrosine phosphorylation of signaling proteins such as Zap70 and Lat in γδT cells (Supplemental Figure 1; supplemental material available online with this article; https://doi.org/10.1172/JCI95837DS1). Interestingly, we noticed that γδT cells exhibited TCR-induced tyrosine phosphorylation of Syk, a tyrosine kinase primarily responsible for signal transduction of the BCR, the Fc receptor, and certain innate receptors (24). Syk and Zap70, which belong to the Syk family kinases, preferentially associate with certain immune receptors in a cell-specific manner and phosphorylate downstream signaling proteins such as Lat and BLNK. It has been recognized that Zap70, but not Syk, is an essential αβTCR proximal kinase required for positive and negative selection of αβT cells (25–27). In the early stage of αβT cell development, Zap70 and Syk play a redundant role (28).

The phosphorylation of both Zap70 and Syk after γδTCR stimulation led us to investigate their role in γδTCR signals. We analyzed γδT cells in Zap70-deficient (*Zap70*$^{-/-}$), Syk-deficient (*Sykb*$^{-/-}$), and Zap70/Syk–doubly deficient (*Zap70*$^{-/-}$ *Sykb*$^{-/-}$) mice. Because the deletion of Syk results in neonatal lethality, we examined γδT cells isolated from the thymus of these mice at E15.5 or at birth (day 0). In the E15.5 thymus, we found that the number of CD3$^+$TCRδ$^+$ γδT cells was comparable between WT and all mutant mice (Figure 1, A and B). On day 0, *Zap70*$^{-/-}$ mice had a normal number of γδT cells in the thymus, whereas *Sykb*$^{-/-}$ and *Zap70*$^{-/-}$ *Sykb*$^{-/-}$ mice showed a drastic reduction in the number of thymic γδT cells, suggesting a critical contribution of Syk to the development of γδT cells.

To assess the effect of Syk and/or Zap70 deficiency on γδTCR signaling pathways, we examined the phosphorylation of the MAP kinases ERK1 and ERK2 upon anti-CD3ε stimulation (Figure 1, C and D). In *Zap70*$^{-/-}$ γδT cells, ERK phosphorylation was mildly decreased (1 minute after stimulation, 16% reduction of mean fluorescence intensity [MFI]) compared with that detected in WT γδT cells. *Sykb*$^{-/-}$ γδT cells showed a substantial reduction in ERK phosphorylation (79% reduction of MFI), whereas it was undetectable in *Zap70*$^{-/-}$ *Sykb*$^{-/-}$ γδT cells. These results indicate a dominant role for Syk, but not Zap70, in γδTCR signaling, despite their functional redundancy. Indeed, the surface expression of CD5, an indicator of in vivo TCR signal strength, was markedly reduced in *Sykb*$^{-/-}$ γδT cells and was nearly undetectable in *Zap70*$^{-/-}$ *Sykb*$^{-/-}$ γδT cells, whereas it remained unaffected in *Zap70*$^{-/-}$ γδT cells (Figure 1E). Taken together, our results demonstrate that Syk is the major γδTCR proximal tyrosine kinase in γδTCR signaling and γδT cell development in the thymus, whereas Zap70 has only a partial contribution.

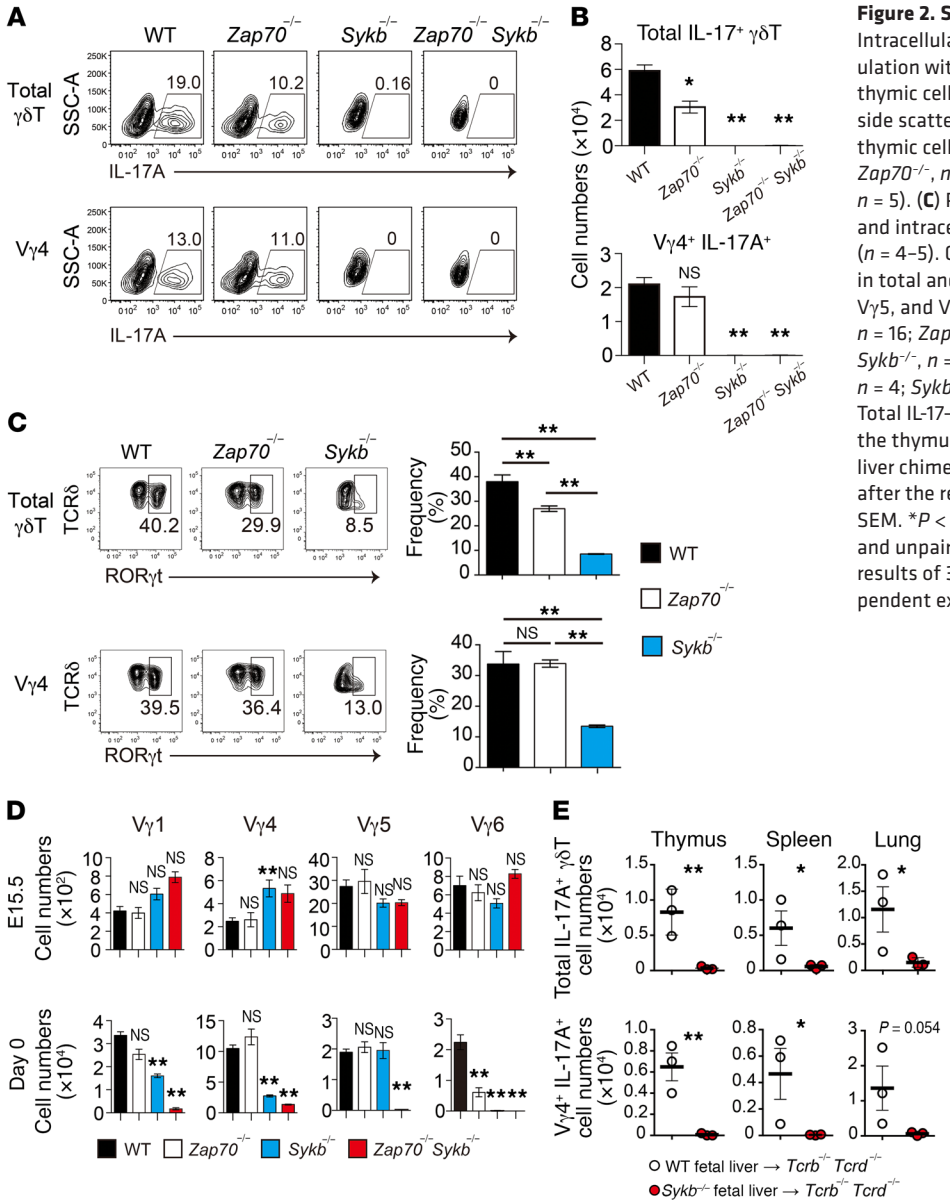

Figure 2. Syk is required for γδT17 development. (**A**) Intracellular staining for IL-17A production after stimulation with PMA and ionomycin in total or Vγ4$^+$ γδT thymic cells from the indicated mice on day 0. SSC-A, side scatter area. (**B**) Total IL-17–producing and Vγ4$^+$ γδT thymic cell numbers per mouse on day 0 (WT, n = 23; *Zap70*$^{-/-}$, n = 4; *Sykb*$^{-/-}$, n = 7; and *Zap70*$^{-/-}$ *Sykb*$^{-/-}$, n = 5). (**C**) Representative profiles for cell-surface TCRδ and intracellular RORγt expression in thymic γδT cells (n = 4–5). Graphs indicate the frequency of RORγt cells in total and Vγ4$^+$ γδT cells. (**D**) Number of Vγ4, Vγ1, Vγ5, and Vγ6 (17D1$^+$Vγ5$^-$) cells per mouse at E15.5 (WT, n = 16; *Zap70*$^{-/-}$, n = 10; *Sykb*$^{-/-}$, n = 8; and *Zap70*$^{-/-}$ *Sykb*$^{-/-}$, n = 2) and on day 0 (WT, n = 19; *Zap70*$^{-/-}$, n = 4; *Sykb*$^{-/-}$, n = 7; and *Zap70*$^{-/-}$ *Sykb*$^{-/-}$, n = 8). (**E**) Total IL-17–producing and Vγ4$^+$ γδT cell numbers from the thymus, spleen, and lungs of the indicated fetal liver chimeric mice. The mice were analyzed 8 weeks after the reconstitution. Data represent the mean ± SEM. *P < 0.05 and **P < 0.01, by 1-way ANOVA (**B**–**D**) and unpaired t test (**E**). Data represent the combined results of 3 independent experiments (**A**–**D**) or 2 independent experiments (**E**).

Syk, but not Zap70, is required for γδT17 development. Subsequently, we examined the functional differentiation of γδT cells in mice at birth, as γδT17 preferentially develops during the late embryonic stage. In the thymus of WT mice on day 0, a substantial fraction (nearly 20%) of γδT cells produced IL-17 upon stimulation with PMA and ionomycin (Figure 2A). The number of γδT17 cells was reduced by approximately 50% in *Zap70*$^{-/-}$ mice (Figure 2, A and B), reflecting a marked reduction in Vγ6$^+$ cells (Figure 2D), which is a prominent subset of γδT17 cells in mice. Another major γδT17 subset, Vγ4$^+$ cells, was unaffected in *Zap70*$^{-/-}$ mice (Figure 2A). In contrast, both *Sykb*$^{-/-}$ and *Zap70*$^{-/-}$ *Sykb*$^{-/-}$ mice showed a complete loss of γδT17, including both Vγ4$^+$ and Vγ6$^+$ cell subsets (Figure 2, A and B). Consistent with these observations, the frequency of γδT cells expressing RORγt, a transcription factor mandatory for IL-17 production, was reduced in *Zap70*$^{-/-}$ and *Sykb*$^{-/-}$ mice (Figure 2C). These results indicate that Syk is essential for γδT17 differentiation and that Zap70 is solely required for the Vγ6$^+$ subset of γδT17 cells.

We detected the expression of all Vγ chains (Vγ1, Vγ4, Vγ5, and Vγ6) in E15.5 fetal thymi from WT, *Zap70*$^{-/-}$, and *Sykb*$^{-/-}$ mice (Figure 2D). Analysis of day-0 neonatal thymus revealed that Zap70 was dispensable for the development of most γδT cells, including Vγ1$^+$, Vγ4$^+$, and Vγ5$^+$ cells, with the exception of Vγ6$^+$ cells. The number of Vγ1$^+$, Vγ4$^+$, and Vγ6$^+$ cells, but not Vγ5$^+$ cells, was significantly reduced in *Sykb*$^{-/-}$ neonatal mice. These Vγ cell subsets were further reduced in number or were nearly absent in *Zap70*$^{-/-}$ *Sykb*$^{-/-}$ mice (Figure 2D). These results indicate the redundant and nonredundant roles of Zap70 and Syk in the development of different neonatal γδT cell subsets: Vγ1$^+$ and Vγ4$^+$ cells require Syk, Vγ5$^+$ cells require either Zap70 or Syk, and Vγ6$^+$ cells require both.

Furthermore, to examine γδT17 development in adult mice, hematopoietic progenitor cells from fetal liver were transplanted into T cell–deficient (*Tcrb*$^{-/-}$ *Tcrd*$^{-/-}$) mice. We observed that WT progenitor cells differentiated into γδT17 cells in the thymus, spleen, and lungs of the reconstituted mice (Figure 2E and Supplemental Figure 2, A and B). However, in mice reconstituted with

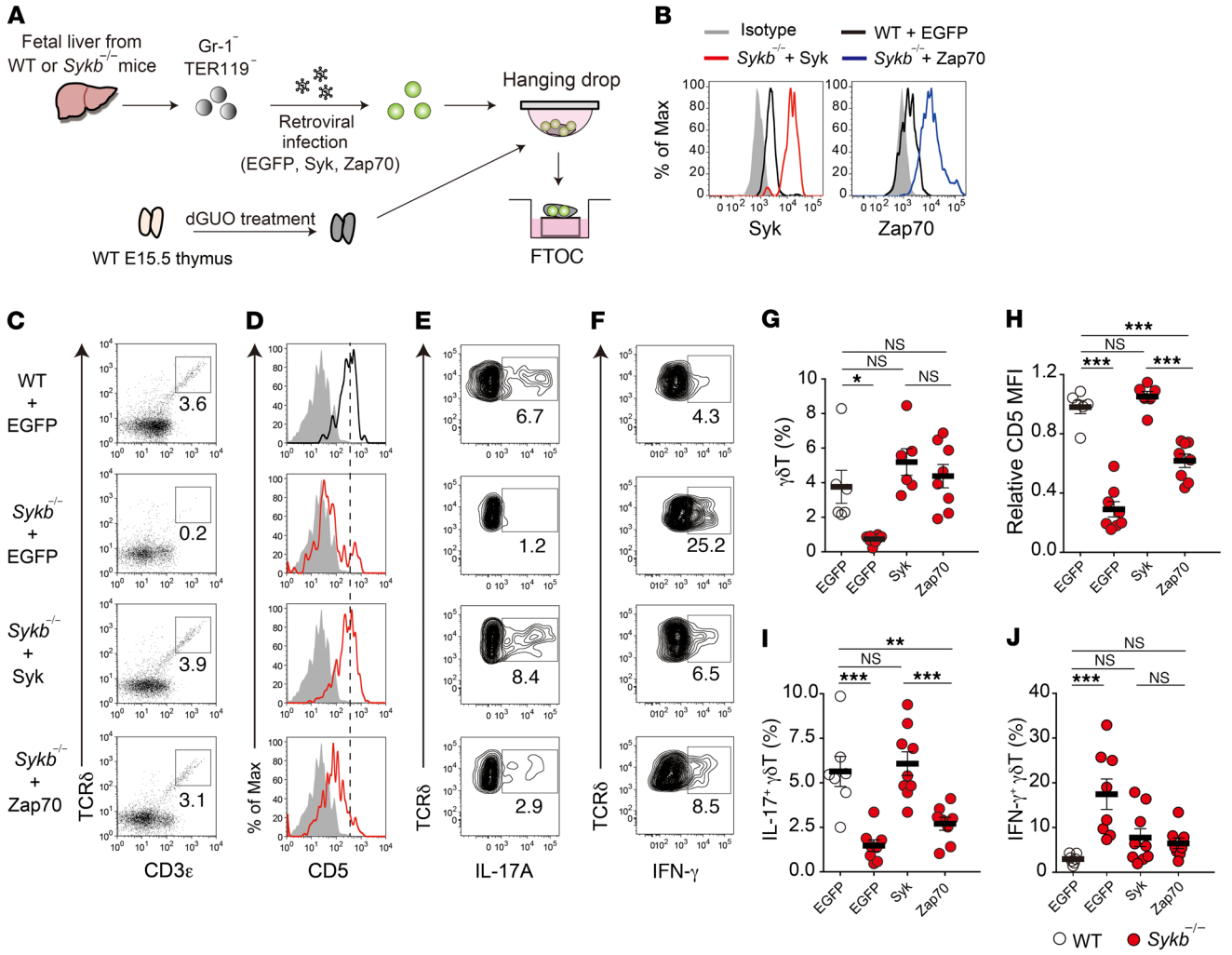

Figure 3. Zap70 fails to functionally substitute Syk in γδT17 development. (**A**) Scheme of the reconstitution of fetal liver T progenitor cells in FTOC. Gr-1$^-$TER119$^-$ fetal liver cells from WT or Syk-deficient mice at E15.5 were infected with retroviruses expressing EGFP alone or Syk or Zap70 along with EGFP. The infected cells were reconstituted in dGUO-treated WT fetal thymic lobes, and the reconstituted thymic lobes were further cultured for 9 to 14 days. (**B**) Expression of Syk and Zap70 in EGFP$^+$CD3ε$^+$TCRδ$^+$ cells from FTOC on day 9. (**C**) Expression of CD3ε and TCRδ in EGFP$^+$ cells on day 9. (**D**) Expression of CD5 in EGFP$^+$ γδT cells on day 9. (**E** and **F**) Intracellular staining for IL-17A and IFN-γ production in EGFP$^+$ γδT cells on day 14. (**G**) Frequency of the total EGFP$^+$ γδT cells shown in **C** (n = 6–8). (**H**) Relative MFI of CD5 expression in the γδT cells shown in **D** (n = 6–8). (**J**) Frequency of the IL-17A$^+$ γδT cells shown in **E** (n = 7–9). (**I**) Frequency of the IFN-γ$^+$ γδT cells shown in **F** (n = 7–9). Graphs indicate the data for individual thymic lobes (circles) and the mean ± SEM. *P < 0.05, **P < 0.01, and ***P < 0.001, by 1-way ANOVA (**G**–**J**). Data represent at least 2 independent experiments.

Syk-deficient fetal liver cells, γδT17 was completely undetectable. These results, along with those in neonatal mice, showed that Syk is required for γδT17 development throughout life.

In contrast, we found that IFN-γ–producing γδT cells were detectable in *Zap70*$^{-/-}$, *Sykb*$^{-/-}$, and *Zap70*$^{-/-}$ *Sykb*$^{-/-}$ mice (Supplemental Figure 3). In agreement with a previous report (29), the IFN-γ–producing potential was detectable in CD4/CD8 double-negative (DN) thymocytes from *Rag2*$^{-/-}$ mice, indicating that immature thymocytes possess an IFN-γ–producing potential in response to certain extracellular stimuli. Given that *Sykb*$^{-/-}$ γδT cell development was arrested at the immature CD5$^-$ stage, we could not investigate the requirement of Syk in γδTCR-mediated IFN-γ production in mature γδT cells upon agonistic ligand stimulation.

Zap70 fails to functionally substitute for Syk in γδT17 development. To clarify the functional difference between Syk and Zap70, we examined whether Syk can be replaced by Zap70 in developing γδT cells. Fetal liver T progenitor cells from *Sykb*$^{-/-}$ mice were infected with retroviruses expressing Syk or Zap70 along with EGFP and seeded into a fetal thymus organ culture (FTOC) (Figure 3A). Compared with WT cells, the retrovirus-infected *Sykb*$^{-/-}$ cells in the FTOC expressed approximately 10-fold higher levels of Syk or Zap70 proteins (Figure 3B). Syk expression clearly recovered γδT cell development from *Sykb*$^{-/-}$ T progenitor cells (Figure 3, C and G). We found that expression of CD5 in γδT cells was also completely restored by Syk expression (Figure 3, D and H). Most important, the differentiation of γδT17 cells was fully restored to WT cell levels (Figure 3, E and I). The overexpression of Zap70 in *Sykb*$^{-/-}$ progenitors also restored the frequency of γδT cells (116% of WT and 84% of Syk expression). However, this overexpression failed to fully induce CD5 expression (63% of WT and 59% of Syk expression levels) and γδT17 development (48% of WT and 44% of Syk expression levels). The frequency of IFN-γ–producing γδT

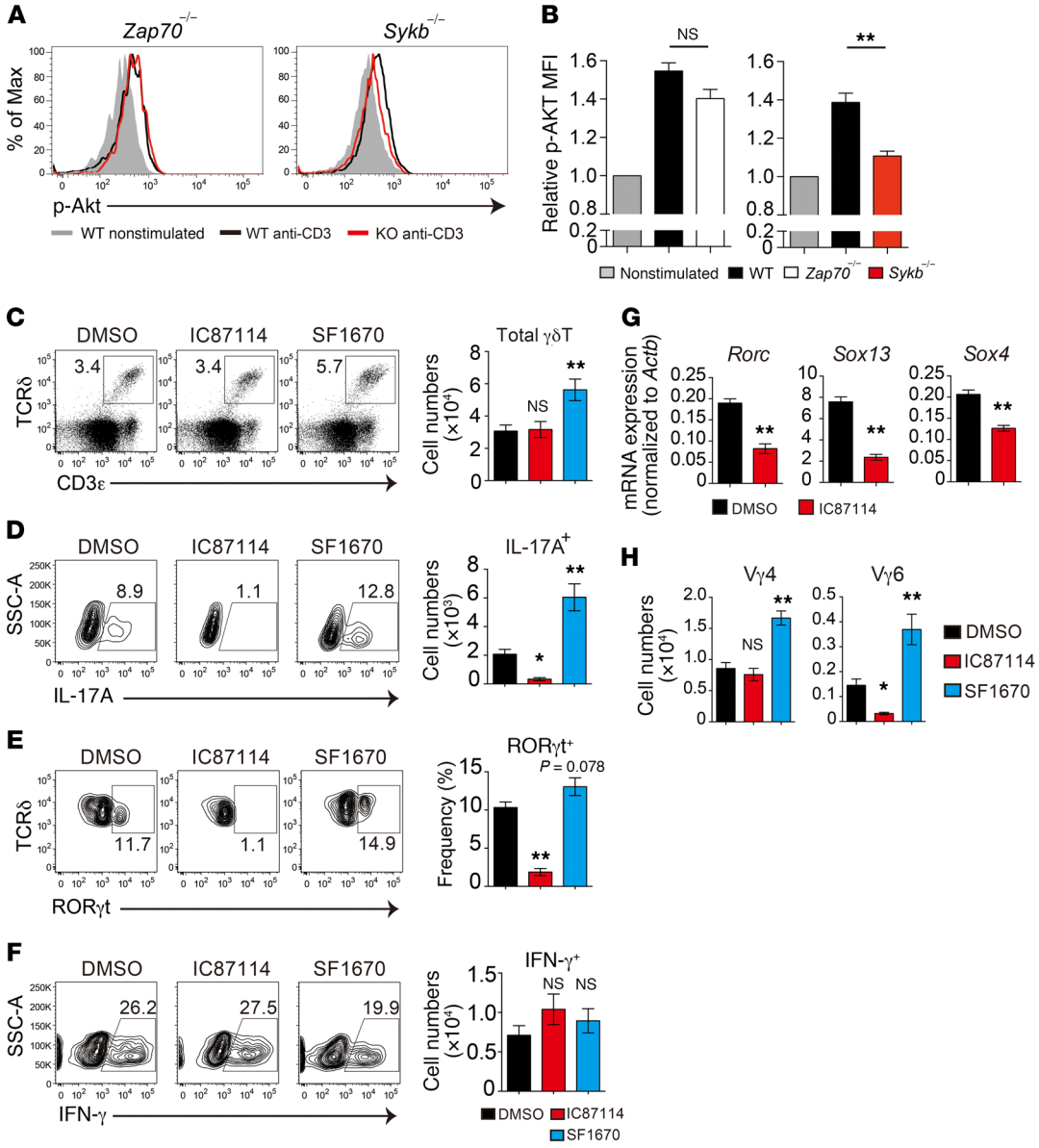

Figure 4. The PI3K pathway controls γδT17 development. (**A** and **B**) TCR-induced Akt phosphorylation in thymic γδT cells from *Zap70*$^{-/-}$ or *Sykb*$^{-/-}$ mice. Histograms show staining profiles of p-Akt in cells from WT (black lines) and mutant (red lines) mice, overlaid with nonstimulated profiles (shaded) after a 1-minute stimulation (**A**). MFI relative to nonstimulated controls (**B**). Thymocytes from adult *Zap70*$^{-/-}$ mice (n = 3) and neonatal *Sykb*$^{-/-}$ mice (n = 4) were used. (**C**–**G**) E15.5 fetal thymus from WT mice was cultured with vehicle alone (DMSO, 0.01%), IC87114 (1 μM), or SF1670 (2.5 μM) for 7 days (n = 5–11). (**C**) Flow cytometric profiles for CD3ε and TCRδ expression and absolute number of γδT cells. (**D**) Intracellular staining profiles for IL-17A production in γδT cells and absolute number of IL-17A–producing γδT cells (per lobe). (**E**) Intracellular staining profiles for RORγt expression in γδT cells and frequency of RORγt$^+$ γδT cells. (**F**) Intracellular staining profiles for IFN-γ production in γδT cells and absolute number of IFN-γ–producing γδT cells (per lobe). (**G**) mRNA expression of *Rorc*, *Sox13*, and *Sox4* in isolated γδT cells. Gene expression was normalized to β-actin (*Actb*) mRNA. (**H**) Number of Vγ4$^+$ and Vγ6$^+$ γδT cells. Data represent the mean ± SEM. *P < 0.05 and **P < 0.01, by unpaired t test (**B** and **G**) and 1-way ANOVA (**C**–**F** and **H**). Data represent 2 independent experiments (**A** and **B**) or a single experiment (**G**), or the combined results of 2 independent experiments (**C**–**F** and **H**).

cells was significantly increased in the absence of Syk but was restored to WT levels by the overexpression of Syk or Zap70 (Figure 3, F and J). These results indicate that, although the expression levels of Zap70 are 10-fold higher than normal levels, Zap70 cannot be a substitute for Syk in γδTCR signal transduction and induction of γδT17 development in *Sykb*$^{-/-}$ γδT cells, suggesting a nonredundant role of Syk in γδTCR signaling.

Requirement of Zap70 in γδT cells. Despite the critical role of Zap70 in αβT cell development, our results showed that its requirement in γδT cell development in the thymus was limited to the Vγ6$^+$ cell subset. We focused on Vγ6$^+$ cells in *Zap70*$^{-/-}$ mice and observed that CD5 expression levels were normal at E15.5. However, these levels were significantly reduced on day 0, suggesting that Zap70 is not essential for initial γδTCR signaling but rather is required for the thymic maturation of Vγ6$^+$ cells, probably via continuous γδTCR signaling (Supplemental Figure 4, A and B). This idea is supported by the fact that the expression levels of Zap70 protein and mRNA were the highest in the Vγ6$^+$ sub-

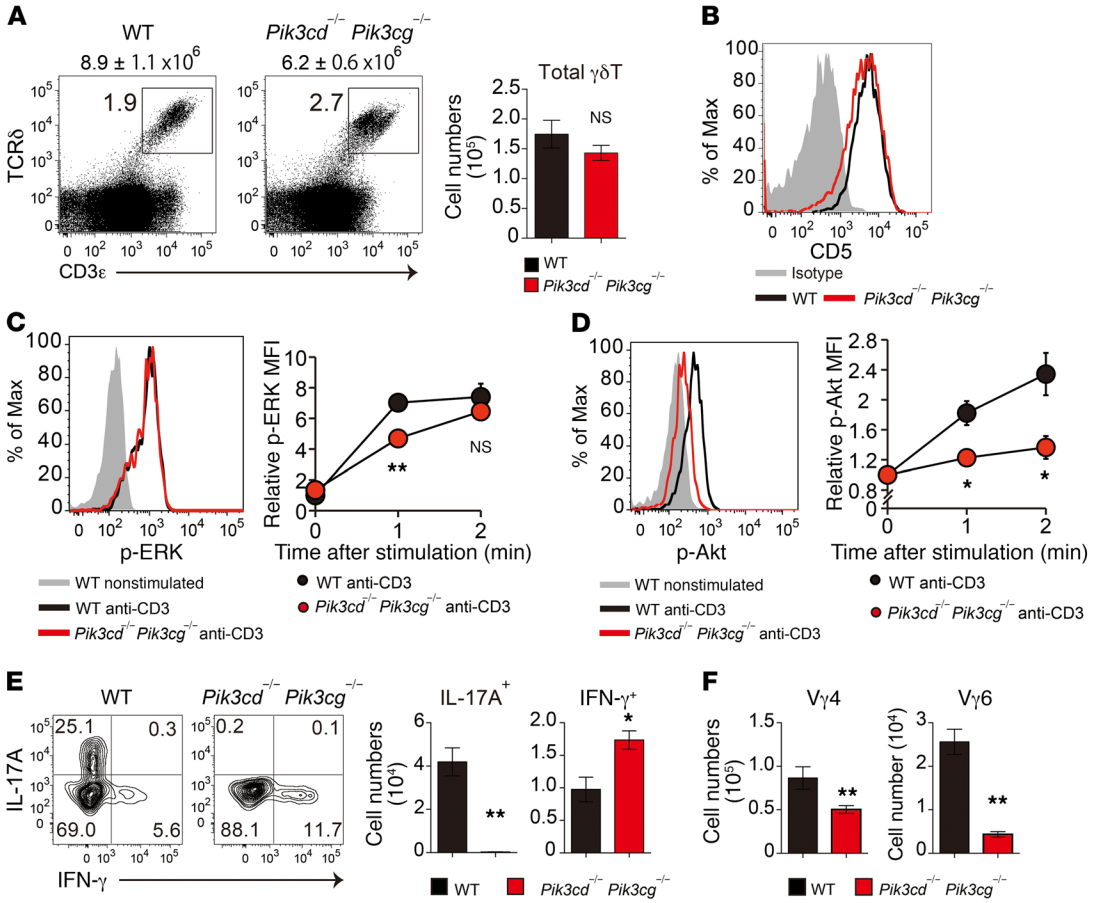

Figure 5. Impaired development of γδT17 cells in PI3K-deficient mice. (**A**) Flow cytometric profiles for CD3ε and TCRδ in total thymocytes from 0-day-old WT and *Pik3cd*$^{-/-}$*Pik3cg*$^{-/-}$ mice. The total number of thymocytes is shown above each flow cytometric plot. Graph indicates the total number of γδT cells per mouse (n = 4–6). (**B**) Flow cytometric analysis of CD5 expression in thymic γδT cells (n = 4–6). (**C** and **D**) TCR-induced ERK (**C**) and Akt (**D**) phosphorylation in thymic Vγ4$^+$ γδT cells from 1-day-old WT and *Pik3cd*$^{-/-}$ *Pik3cg*$^{-/-}$ mice. Graphs indicate the MFI relative to the nonstimulated control. (**E**) Intracellular staining for IL-17A and IFN-γ production in neonatal thymic γδT cells from 0-day-old WT and *Pik3cd*$^{-/-}$ *Pik3cg*$^{-/-}$ mice after stimulation with PMA and ionomycin. The number of IL-17A$^+$ and IFN-γ$^+$ γδT cells per mouse is shown (n = 3–6). (**F**) Number of Vγ4$^+$ and Vγ6$^+$ γδT cells (per mouse) in the indicated mice (n = 4–6). All data represent the mean ± SEM. *P < 0.05 and **P < 0.01, by 2-way ANOVA (**C** and **D**) and unpaired t test (**A**, **E**, and **F**). Data represent a single experiment using more than 7 neonatal mice per group.

set among γδT cells (Supplemental Figure 4C). These results are in agreement with previous findings that Vγ6$^+$ cell development is impaired in mutant mice harboring a hypomorphic *Zap70* mutation (30). Zap70 is also required for peripheral Vγ4$^+$ cells, including the γδT17 subset, as well as for IFN-γ–producing γδT cells in the spleen and lungs (Supplemental Figure 4, D and E). In contrast, the Vγ1$^+$ cell subset was normal or increased in the periphery of *Zap70*$^{-/-}$ mice. Although it still remained unclear why peripheral Vγ4$^+$ γδT cells were reduced in *Zap70*-deficient mice, it is possible that Zap70-dependent TCR signals support the survival and/or migration of these cells. Thus, the requirement of Zap70 in γδT cell development is limited to the thymic maturation of Vγ6$^+$ cells and peripheral maintenance of Vγ4$^+$ cells.

The PI3K/Akt pathway controls γδT17 development. These results prompted us to examine the unique function of Syk in γδTCR signaling and γδT17 development. Previous studies showed that Syk is recruited to the BCR and Fcε receptor for the activation of PI3K in B cells and mast cells, respectively (31). The activated PI3K produces phosphatidylinositol (3,4,5)-trisphosphate (PIP3), which in turn activates downstream protein kinases including Akt, PDK1, and Tec. The level of PIP3 is negatively regulated through its hydrolysis catalyzed by PTEN, a phosphoinositide phosphatase. In αβT cells, αβTCR signal–induced activation of the PI3K/Akt pathway requires CD28 costimulation (32), whereas in γδT cells, the γδTCR signal can induce Akt phosphorylation in the absence of costimulatory signals (19).

Although Akt phosphorylation induced by γδTCR stimulation was not altered in *Zap70*$^{-/-}$ γδT cells, it was significantly reduced in *Sykb*$^{-/-}$ γδT cells compared with WT γδT cells (Figure 4, A and B). We found that γδTCR-induced Akt phosphorylation, but not ERK phosphorylation, was completely inhibited by treatment with IC87114, an inhibitor of the p110δ catalytic subunit of PI3K (Supplemental Figure 5, A and B). This finding indicates that Akt activation depends on PI3K in γδTCR signaling. These results demonstrate that Syk plays a critical role in γδTCR-induced activation of the PI3K/Akt pathway.

To examine the roles of PI3K and PTEN in γδT cell development, we cultured E15.5 fetal thymus from WT mice with IC87114 or SF1670, an inhibitor of PTEN. After 7 days of FTOC, the develop-

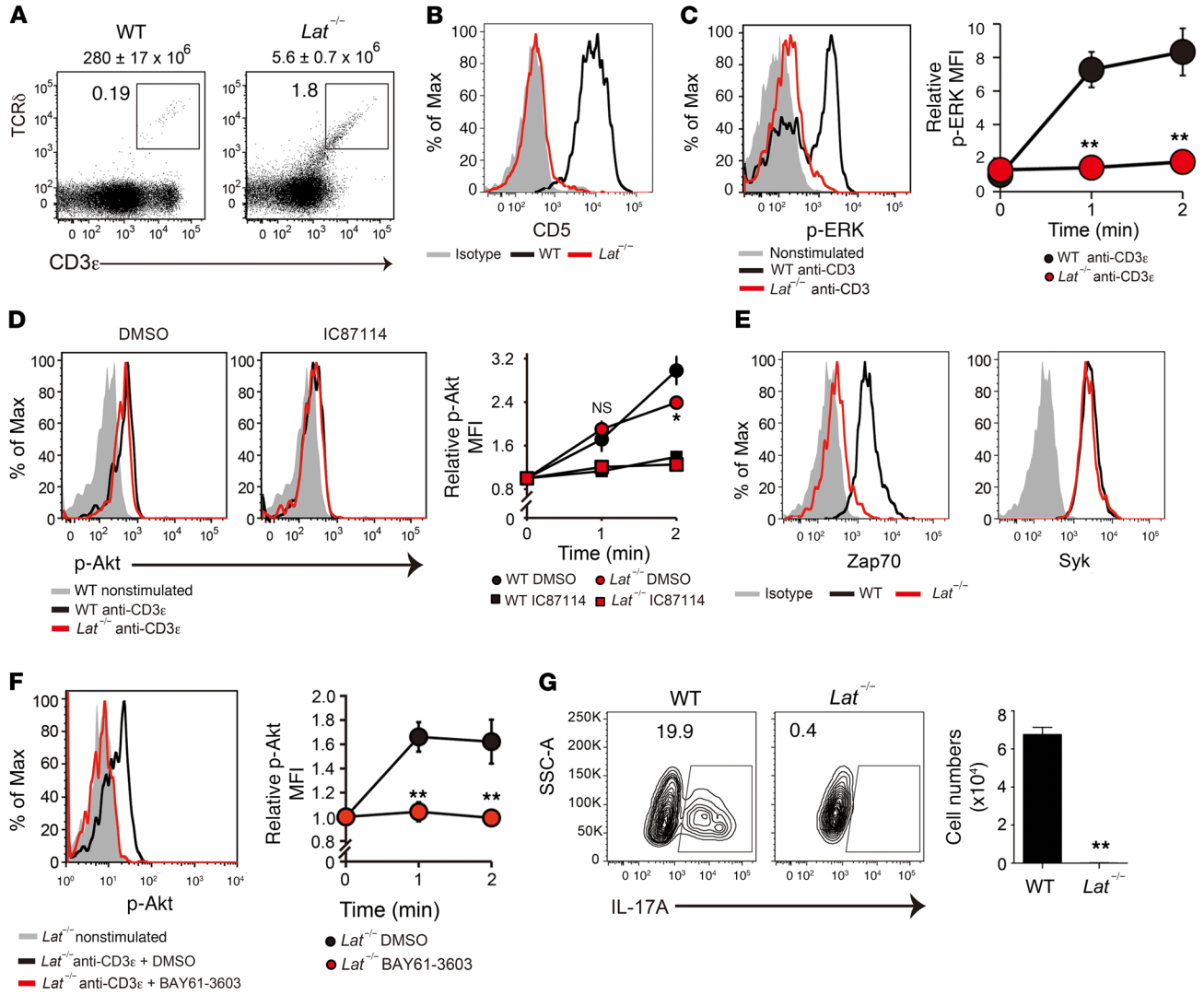

Figure 6. Syk mediates the Lat-independent TCR signal to the PI3K/Akt pathway. (**A**) Flow cytometric profiles for CD3ε and TCRδ in total thymocytes from 5-week-old WT and *Lat*$^{-/-}$ mice. The total number of thymocytes is shown above each flow cytometric plot (n = 3). (**B**) Flow cytometric analysis of CD5 expression in thymic γδT cells (n = 3). (**C**) TCR-induced ERK phosphorylation in thymic γδT cells. Graph indicates the MFI relative to the nonstimulated control (n = 3). (**D**) TCR-induced Akt phosphorylation in thymic γδT cells pretreated or not with IC87114 (10 μM). Graph shows the MFI relative to the nonstimulated control (n = 3). (**E**) Flow cytometric analysis of Zap70 and Syk expression in thymic γδT cells from 5-week-old WT and *Lat*$^{-/-}$ mice (n = 3). (**F**) TCR-induced Akt phosphorylation in *Lat*$^{-/-}$ γδT cells pretreated or not with BAY61-3606 (10 μM). Graph shows the MFI relative to the nonstimulated control (n = 3). (**G**) Intracellular staining for IL-17A production in neonatal thymic γδT cells from WT mice (n = 3) and *Lat*$^{-/-}$ mice (n = 5) after stimulation with PMA and ionomycin. The number of IL-17A$^+$ γδT cells (per mouse) is shown. All data represent the mean ± SEM. *P < 0.05 and **P < 0.01, by 2-way ANOVA (**C**, **D**, and **F**) and unpaired t test (**G**). Data represent 2 independent experiments (**A**, **B**, **D**, **F**, and **G**) or a single experiment (**C** and **E**).

ment of γδT17 cells and RORγt-expressing γδT cells was drastically impaired by treatment with IC87114, although the total number of γδT cells and IFN-γ–producing γδT cells was not decreased (Figure 4, C–F). We also found that IC87114 reduced the mRNA expression of *Rorc*, *Sox13,* and *Sox4*, the transcription factors essential for γδT17 induction, in γδT cells (Figure 4G). In contrast, we found that the number of γδT17 cells and RORγt-expressing γδT cells was increased by SF1670 treatment, whereas the number of IFN-γ–producing γδT cells was normal (Figure 4, D–F). Vγ6$^+$ cell numbers were significantly reduced by IC87114 and increased by SF1670 treatment, while Vγ4$^+$ cell numbers were increased by SF1670 (Figure 4H).

We further investigated the in vivo role of the PI3K pathway in γδT cell development, using mice doubly deficient in the PI3K catalytic subunits p110γ and p110δ (*Pik3c*$^{-/-}$ *Pik3cd*$^{-/-}$). The *Pik3cg*$^{-/-}$ *Pik3cd*$^{-/-}$ mice had a normal total number of γδT cells and CD5 expression in γδT cells in neonatal thymus (Figure 5, A and B), indicating that PI3K is not required for γδTCR signaling or thymic γδT cell development. ERK phosphorylation occurred in response to γδTCR stimulation (Figure 5C), although γδTCR-induced Akt phosphorylation was severely impaired in *Pik3cg*$^{-/-}$ *Pik3cd*$^{-/-}$ γδT cells (Figure 5D). These γδT cells showed a complete loss of IL-17–producing capacity (Figure 5E) and a significant reduction in Vγ4$^+$ and Vγ6$^+$ subsets (Figure 5F). Notably, we found that the development of IFN-γ–producing γδT cells was not impaired in *Pik3cg*$^{-/-}$ *Pik3cd*$^{-/-}$ mice (Figure 5E), indicating the specific requirement of PI3K in γδT17 development.

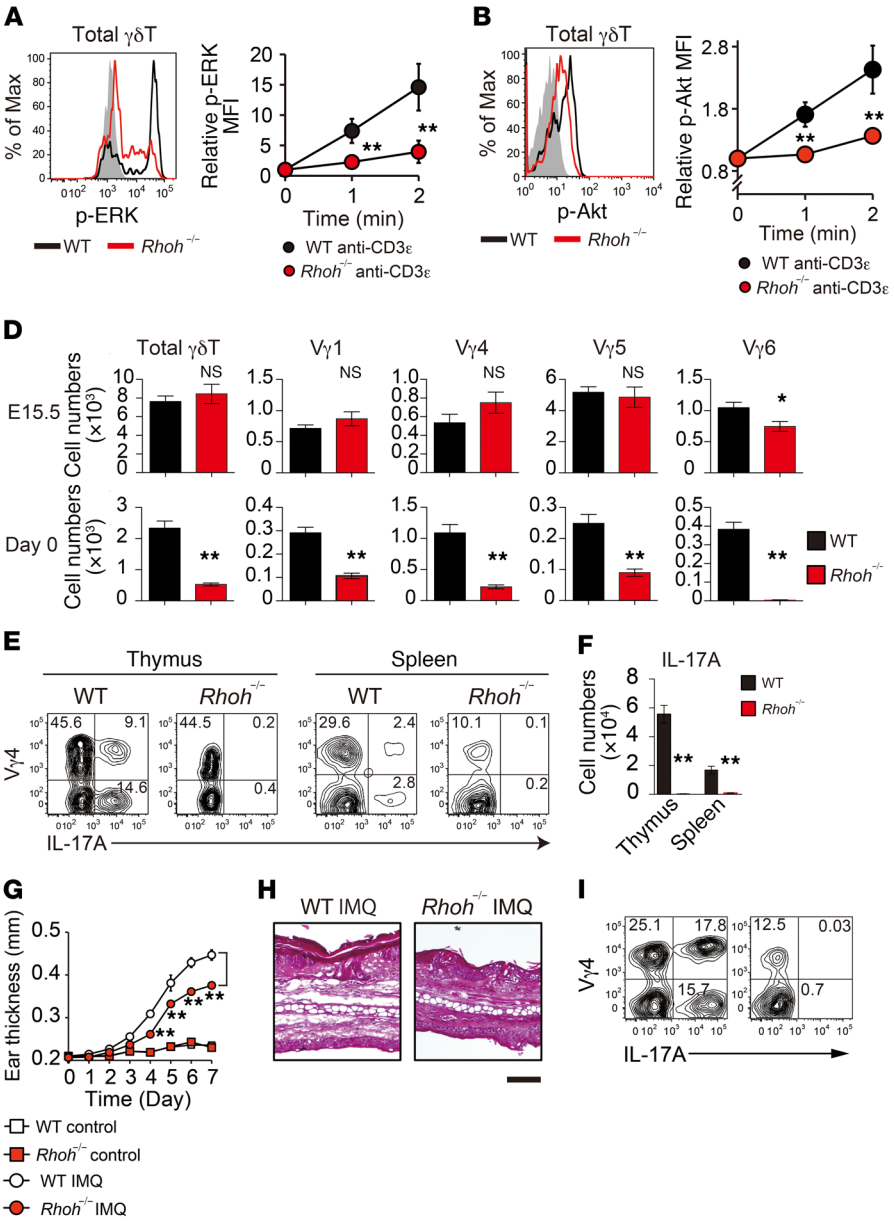

Figure 7. RhoH mediates the γδTCR signaling required for γδT17 development. (**A** and **B**) TCR-induced ERK and Akt phosphorylation in thymic γδT cells from WT (n = 3) and *Rhoh*$^{-/-}$ mice (n = 3). (**C**) Representative CD5 expression profiles in thymic γδT cells (n = 3). (**D**) Number of cells in the indicated thymic γδT subsets from WT and *Rhoh*$^{-/-}$ mice at E15.5 (WT, n = 5; *Rhoh*$^{-/-}$, n = 5) and on day 0 (WT, n = 8; *Rhoh*$^{-/-}$, n = 9). (**E** and **F**) Staining for Vγ4 and IL-17A in thymic (day 0; WT, n = 4; *Rhoh*$^{-/-}$, n = 4) and splenic (6-week-old; WT, n = 8; *Rhoh*$^{-/-}$, n = 8) γδT cells after stimulation with PMA and ionomycin. Graph shows the quantification of IL-17A$^+$ γδT cells (per mouse). (**G**–**I**) WT and *Rhoh*$^{-/-}$ mice were treated daily for 7 days with IMQ cream or control cream on the ear (n = 3). Kinetics of IMQ-induced ear swelling (**G**), representative H&E staining of ear sections on day 7 (**H**), and flow cytometric analysis of IL-17A$^+$ cells in γδT cells from ear-draining lymph nodes on day 7 (**I**). Scale bar: 100 μm. All data represent the mean ± SEM. $^*P < 0.05$ and $^{**}P < 0.01$, by 2-way ANOVA (**A**, **B**, and **G**)and unpaired t test (**D** and **F**). Data represent more than 2 independent experiments (**A**–**F**) or a single experiment (**G**–**I**).

These results indicate that the PI3K/Akt pathway downstream of Syk-mediated γδTCR signal controls γδT17 development.

Syk mediates Lat-independent, noncanonical signaling to the PI3K/Akt pathway. How does Syk activate the PI3K/Akt pathway in γδTCR signaling? Lat is known to be a direct substrate of Zap70 and Syk kinases, acting as a scaffold for downstream signaling molecules. We examined the γδT cell signaling and developmental potential of Lat-deficient (*Lat*$^{-/-}$) mice. As reported previously (33), *Lat*$^{-/-}$ mice showed a complete arrest of γδT cell development at the precursor stage, as characterized by the extremely low number of γδTCR$^+$ cells and the absence of CD5 expression (Figure 6, A and B). Anti-CD3ε–induced ERK phosphorylation was also undetectable in *Lat*$^{-/-}$ γδT cells (Figure 6C). Interestingly, we found that Akt phosphorylation levels were normal in anti-CD3–stimulated *Lat*$^{-/-}$ γδT cells (Figure 6D). This Akt activation was inhibited by treatment with IC87114, indicating that the PI3K/Akt signaling axis is independent of the Lat-mediated pathway.

Previous studies have shown that the expression of Zap70 and Syk is inversely regulated during αβT cell development in the thymus; Zap70 is hardly detectable at the DN1–3 stages, increases thereafter, and reaches the maximum level in mature αβT cells, while Syk is robustly expressed at the DN1–3 stages, gradually decreases thereafter, and reaches an undetectable level at the mature stage (34). In γδT cells, Syk protein expression is detectable even at the mature stage (35). In agreement with these previous data, we found that Zap70 expression was almost undetectable in *Lat*$^{-/-}$ γδT cells, which showed developmental arrest at the DN3 stage. Syk expression was almost comparable between WT and *Lat*$^{-/-}$ γδT cells, indicating that γδTCR signals solely depended on Syk at this stage (Figure 6E). Notably, pretreatment with BAY61-3606, a specific inhibitor of Syk, significantly reduced γδTCR-induced Akt phosphorylation in *Lat*$^{-/-}$ γδT cells (Figure 6F). These results indicate that γδTCR-induced PI3K/Akt activation depends on Syk but not Lat. Although the PI3K/Akt pathway was intact,

Lat$^{-/-}$ γδT cells had no potential to produce IL-17, indicating that the Lat-independent PI3K/Akt pathway is not sufficient for γδT17 differentiation (Figure 6G).

Collectively, our results suggest that γδTCR-induced Syk activation stimulates the Lat-dependent canonical pathway, including the Ras/MAPK cascade, and the Lat-independent noncanonical pathway mediated by the PI3K/Akt axis. The former serves as a mainstream signal for γδT cell differentiation from precursor cells, whereas the latter induces the additional program toward γδT17 differentiation.

The adaptor protein RhoH mediates the γδTCR signaling required for γδT17 development. Previously, we and other groups have reported that Zap70 and Syk require the receptor proximal adaptor protein RhoH for their recruitment to the αβTCR in T cells and the Fcε receptor in mast cells, respectively, and that RhoH is essential for the optimal activation of these receptor signals (36, 37). Subsequently, we investigated whether the γδTCR signals also require RhoH-mediated kinase recruitment. γδT cells from RhoH-deficient (*Rhoh*$^{-/-}$) mice had a marked reduction in γδTCR stimulation–induced ERK and Akt phosphorylation, indicating that RhoH is required for γδTCR signal transduction (Figure 7, A and B). Indeed, the expression of CD5 in γδT cells was markedly reduced in *Rhoh*$^{-/-}$ mice (Figure 7C). We found that the neonatal development of Vγ4$^+$ and Vγ6$^+$ γδT17 cells was also significantly impaired in *Rhoh*$^{-/-}$ mice (Figure 7D). These γδT cell phenotypes recapitulated those of *Sykb*$^{-/-}$ mice, strongly suggesting that RhoH mediates the γδTCR/Syk signaling axis for the induction of γδT17 development.

Last, we assessed the in vivo significance of RhoH/Syk-mediated γδTCR signals using *Rhoh*$^{-/-}$ mice and found that Vγ4$^+$ γδT cell numbers were markedly reduced, while Vγ6$^+$ γδT cells were barely detectable in the thymus throughout ontogeny (Supplemental Figure 6, A and B). In adult *Rhoh*$^{-/-}$ mice, Vγ4$^+$ and Vγ6$^+$ γδT cell numbers were significantly reduced in peripheral tissues, whereas the total numbers of γδT cells and Vγ1$^+$ (spleen and lung), Vγ5$^+$ (skin), and Vγ7 (small intestine) cell subsets were comparable to those in WT mice (Supplemental Figure 6C). In particular, we did not detect γδT17 cells in the thymus or periphery in *Rhoh*$^{-/-}$ mice (Figure 7, E and F). On the other hand, we found that thymic development of IFN-γ–producing γδT cells was unimpaired in *Rhoh*$^{-/-}$ mice (Supplemental Figure 3). Previous studies have demonstrated that Vγ4$^+$ γδT17 cells play a crucial role in psoriasis-like dermatitis induced by imiquimod (IMQ). Upon IMQ treatment, Vγ4$^+$ γδT17 cells specifically expand in the draining lymph node and recirculate to inflamed skin (4, 38). We observed that IMQ-induced skin inflammation was significantly attenuated and that the induced increase in Vγ4$^+$ γδT17 cells was completely undetectable in *Rhoh*$^{-/-}$ mice (Figure 7, G–I). A similar attenuation of inflammation was also observed in mice reconstituted with Syk-deficient fetal liver cells (Supplemental Figure 2C). These results indicate that a deficiency of RhoH-mediated γδTCR signals has a marked impact on the γδT17-mediated inflammatory response in vivo.

Discussion

In this study, we explored the molecular mechanisms of γδTCR signaling pathways for the development and effector fate decision of γδT cells during thymic development, focusing on the role of the receptor proximal tyrosine kinase Syk. Early pioneering studies demonstrated that Syk is required for the development of certain γδT cell subsets such as skin- or intestine-resident γδT cells (35, 39). However, the functional significance of Syk in the repertoire formation and effector function of γδT cells has not been addressed to date. The present study revealed that Syk-dependent γδTCR signals are indispensable for the thymic maturation and acquisition of the effector function of γδT cells.

It has been demonstrated that the TCR signaling machinery differs between αβT and γδT cells (17–23, 40), although these 2 cell types derive from common progenitors in the thymus. We showed here that in ex vivo γδT cells, engagement of the γδTCR-CD3 complex leads to the phosphorylation of Syk and Zap70. Experiments using gene-deficient mice proved that Syk plays a dominant role in γδTCR signaling. Unexpectedly, it was found that Zap70 has a limited contribution to γδTCR signaling and is dispensable for the thymic development of most γδT cells. This markedly contrasts αβTCR signaling and αβT cell development, both of which completely depend on Zap70 but not Syk (25–27). Taken together, these observations indicate that, unlike αβT cells that use the αβTCR/Lck/Zap70 axis, γδT cells use Syk as a dominant γδTCR proximal kinase to initiate downstream signaling cascades. This suggests a common feature of antigen receptor signaling machinery between γδT and B cells rather than αβT cells.

Why do γδT cells preferentially rely on Syk to drive γδTCR signals? It may be at least partly explained by the differential expression of Syk and Zap70 during T cell development (34). We found high Syk and low Zap70 expression in immature γδT cells (such as γδT cells from *Lat*$^{-/-}$ mice), which might account for the dominant role of Syk rather than Zap70 in the early phase of γδT cell development. While αβT cells lose Syk expression during development (34), γδT cells maintain Syk expression until the mature stage (35). In addition to the quantitative difference, the qualitative difference between Syk and Zap70 may be the cause of their differential requirement. Indeed, our experiments with FTOC demonstrated that the overexpression of Zap70 in Syk-deficient T progenitor cells did not fully restore γδTCR signaling and γδT17 development. A previous report also showed that the ectopic expression of Zap70 in Syk-deficient BM macrophages fails to restore the differentiation into normal osteoclasts (41). The functional incompetence of Zap70 compared with Syk may be explained by the differential behavior of these kinases. The kinase domain of Zap70 has been shown to exert lower catalytic activity than that of Syk (42). It is also possible that Syk and Zap70 have different specificities to target proteins, because the ectopic expression of Syk in human αβT cells can result in altered gene expression downstream of TCR signaling (43). The Src homology 2 (SH2) domains of Syk may be more structurally flexible than those of Zap70 (44), possibly leading to a higher accessibility of Syk to the immunoreceptor tyrosine–based activation motifs (ITAMs) in γδTCR-CD3 complexes. Furthermore, although the activation of Zap70 depends on Lck, Syk functions in an Lck-independent manner (45). These differential properties of the 2 kinases are likely to explain the preferential requirement of Syk in γδTCR signaling.

It is likely that the most important target of Syk in γδT cells is Lat, which forms a signalosome that provides docking sites for SH2-containing proteins such as PLCγ. This leads to activation of the

Ras/MAPK, Ca/NFAT, and PKCθ/NF-κB pathways (16). Our results, along with those of a previous study (33), indicate that *Lat*$^{-/-}$ γδT cells show a complete loss of MAPK activation, no signs of maturation, and no γδT17 induction. However, our finding that Akt phosphorylation upon γδTCR stimulation was not altered in *Lat*$^{-/-}$ γδT cells clearly indicates that the γδTCR/PI3K/Akt axis is independent of the Lat signalosome. A previous study using cell-free experiments showed that Syk directly binds to the p85α regulatory subunit of PI3K (46). In B cells, upon BCR stimulation, Syk phosphorylates BCAP, an adaptor protein that interacts with and activates PI3K (47). Activation of the PI3K/Akt pathway in αβT cells is mediated by the binding of PI3K to the phosphorylated cytoplasmic domain of CD28 upon interaction with its ligands, CD80 or CD86 (48). This mechanism explains the requirement of costimulatory signals from antigen-presenting cells in αβT cell activation. Our data indicate that γδTCR signals can directly activate the PI3K/Akt pathway, probably through direct interaction between Syk and PI3K proteins or in an indirect manner, mediated by putative adaptor protein(s). Uncovering the molecular links between Syk and PI3K in γδT cells still remains a challenge.

Collectively, Syk-mediated γδTCR signals can activate the canonical pathway, in which the Lat signalosome acts as a platform for the activation of downstream cascades, as well as the noncanonical accessory pathway mediated by the PI3K/Akt axis. We infer that the latter enables γδT cells to efficiently respond to antigen recognition without costimulatory signals.

We further elucidated the essential role of the PI3K/Akt pathway in γδT17 development. The induction of γδT17 cells was significantly repressed by pharmacological inhibition or genetic ablation of PI3K and enhanced by PTEN inhibition, indicating that the production of PIP3 is a critical determinant of γδT17 cell differentiation during thymic development. Inhibition of PI3K reduced the expression of the transcription factors RORγt, Sox13, and Sox4 in the developing γδT cells. Hence, the PI3K/Akt pathway plays a crucial role in the transcriptional program toward the γδT17 lineage. Similarly, the PI3K/Akt pathway directs the differentiation of IL-17–producing Th17 cells (49), suggesting that the PI3K/Akt pathway is a common regulatory system shared by αβT and γδT lineages to induce the differentiation program toward IL-17–producing subsets. A previous study showed that the genetic deficiency or pharmacological inhibition of PI3K attenuates γδT17-dependent inflammation (50), highlighting the physiological importance of this signaling pathway in properly mounting the inflammatory potentials.

In conclusion, we describe the significance of Syk-mediated TCR signaling in the physiological development and effector differentiation of γδT cells. Syk acts as a dominant γδTCR proximal tyrosine kinase that activates the canonical signaling cascades mediated by the Lat signalosome as well as the Lat-independent noncanonical signal for activation of the PI3K/Akt pathway for γδT17 induction (Supplemental Figure 7). Elucidating the functional difference between Syk and Zap70 in terms of T cell function as well as their evolutionary history and contribution to pathogenesis would be intriguing for future studies.

Methods

Mice. C57BL/6 mice were purchased from Japan SLC. *Zap70*$^{-/-}$ (25), *Rag2*$^{-/-}$ (51), *Rhoh*$^{-/-}$ (37), *Tcrb*$^{-/-}$ (52), and *Tcrd*$^{-/-}$ (53) mice were described previously. *Sykb*$^{-/-}$, *Lat*$^{-/-}$, *Zap70*$^{-/-}$ *Sykb*$^{-/-}$, and *Pik3cg*$^{-/-}$ *Pik3cd*$^{-/-}$ mice were generated by the CRISPR/Cas9-mediated genome editing method. All mice were bred and maintained under specific pathogen–free conditions in our animal facility and were euthanized by overdose of inhalation anesthetics.

Antibodies. Monoclonal antibodies against CD4 (GK1.5), CD5 (53-7.3), CD8α (53-6.7), CD25 (PC61.5), TCRβ (H57-597), and RORγt (B2D) were purchased from eBioscience. Monoclonal antibodies against CD3ε (17A2), CD44 (IM7), CD11b (M1/70), CD11c (N418), B220 (RA3-6B2), CD49b (DX5), Gr-1 (RB6-8C5), TER-119 (TER-119), TCRδ (GL3), TCR-Vγ1 (2.11), TCR-Vγ4 (UC3-10A6), TCR-Vγ5 (clone 536), IL-17A (TC11-18H10.1), IFN-γ (XMG1.2), Zap70 (1E7.2), Syk (5F5), and Lat (11B.12) were purchased from BioLegend. Monoclonal antibodies against phosphorylated ERK (p-ERK) (197G2) and p-Akt (D9E) were purchased from Cell Signaling Technology. The monoclonal antibody 17D1, specific for TCR-Vγ6/Vδ1 and TCR-Vγ5/Vδ1, was provided by Robert E. Tigelaar (Yale University, New Haven, Connecticut, USA) and used as described previously (54). Anti-Vγ7 monoclonal antibody (GL1) was provided by the late Leo Lefrançois (University of Connecticut Health Center, Farmington, Connecticut, USA) (55). The γδT cell subsets (according to the Heilig and Tonegawa nomenclature) examined in this study are listed in Supplemental Table 1.

Flow cytometry and cell sorting. Flow cytometric analysis and cell sorting were performed with FACSCanto II and FACSAria III systems (BD Biosciences). Prior to cell staining, the Fc blocker (anti-mouse CD16/CD32; clone 2.4G2; TONBO Biosciences) was used. Cells were stained with a mixture of the antibodies at a final concentration of 1 to 2 μg/ml. 7-Aminoactinomycin D (7AAD) was used to exclude dead cells. For intracellular staining, cells were fixed with IC Fixation Buffer (eBioscience) for 30 minutes and stained with antibodies.

CRISPR/Cas9-mediated genome editing in mice. The preparation of single-guide RNA (sgRNA) and Cas9 mRNA was described previously (56). sgRNA and Cas9 mRNA were injected into the cytoplasm of pronuclear-stage eggs from C57BL/6 mice, and the eggs were transferred into the oviducts of pseudopregnant female ICR mice. The target sequences containing PAM sequences (underlined) were as follows: *Zap70*, GGCACGTACGCCATCGCGGGCGG; *Sykb*–1, CACACCACTACACCATCGAGAGG; *Sykb*–2, GCCCAAGACCGGACCCTTTGAGG; *Lat*–1, ACTCACGGCAGCGCACGCACAGG; *Lat*–2, AGGAAACAGCAGGTGTTCGGGGG; *Pik3cg*–1, GTACGTGTCGCTGTACCACGTGG; *Pik3cg*–2, GATCAAAGTGCTTTGGACGTTGG; *Pik3cd*–1, GTGCGGAAGTCGTTTACTTCCGG; *Pik3cd*–2, TCTGCTCATCCCGCATAGCAAGG.

Fetal liver chimeric mice. E15 fetal liver cells were i.v. injected into x-ray–irradiated (4 Gy) *Tcrb*$^{-/-}$ *Tcrd*$^{-/-}$ mice. Mice were analyzed 8 weeks after the transplantation.

Retroviral infection. cDNA fragments encoding Zap70 or Syk were inserted into the retroviral vector pMSCV-IRES-EGFP. Plat-E packaging cells were transfected with the retrovirus plasmid, and its supernatant was used for hematopoietic progenitor cell infection. To obtain hematopoietic progenitor cells, Gr-1^{-}TER119^{-} cells derived from E15.5 fetal livers were cultured in RPMI 1640 complete medium in the presence of IL-7 (25 ng/ml) and stem cell factor (SCF) (50 ng/ml) for 24 hours. The cells were then infected with retrovirus by the spin-infection method as described previously (57).

FTOC. Thymic lobes isolated from E15.5 fetuses were cultured as previously described (57). IC87114 (SYNkinase) or SF1670 (Milli-

poreSigma) were added into culture medium at 1 μM or 2.5 μM, respectively. For reconstitution with retrovirally transduced T progenitor cells, E15.5 thymic lobes were cultured with 1.35 mM deoxyguanosine (dGuo) for 5 days. The dGuo-treated thymic lobes were incubated with retrovirus-infected fetal liver cells in hanging-drop culture for 24 hours, rinsed with culture medium, and further cultured in normal FTOC.

Preparation of tissue-resident lymphocytes. To prepare lung- and skin-resident lymphocytes, lung or ear tissue from adult mice was minced into small pieces and digested with 0.2% collagenase D (Roche) and 0.01% DNase I (Roche) at 37°C for 30 minutes. The digested tissues were disrupted by using a syringe and 18-gauge needle, and cells were passed through a 100-mm nylon mesh to remove tissue debris. The enzymatic reaction was stopped by adding PBS containing 2 mM EDTA and 2% FCS. To prepare the small intestine cell suspension, gut fragments from which Payer's patches were removed were cut open and incubated for 30 minutes at 4°C in PBS containing 30 mM EDTA. After incubation, the gut fragments were washed with PBS and then vigorously shaken to collect the small intestine epithelial fraction. Leukocytes from the intestine epithelial fraction were isolated with a 40%–80% Percoll gradient.

Quantitative mRNA analysis. Total RNA was extracted from isolated cells using the RNeasy Kit (QIAGEN) and reverse transcribed with SuperScript III (Invitrogen, Thermo Fisher Scientific). Quantitative PCR was performed with SYBR Premix ExTaq (TaKaRa) and the StepOne Real-Time PCR System (Life Technologies, Thermo Fisher Scientific). The results were normalized to β-actin expression levels.

Cell stimulation. Total thymocytes or purified γδT cells (1×10^6 to 5×10^6) were preincubated in RPMI 1640 complete medium at 37°C for 5 minutes and then added to an equal volume of RPMI 1640 complete medium containing biotinylated anti-CD3ε antibody (60 μg/ml; 145-2C11; BioLegend) and streptavidin (21 μg/ml; SouthernBiotech). When necessary, cells were preincubated with IC87114 or BAY61-3603 (MilliporeSigma) at 37°C for 1 hour prior to stimulation. For FACS analysis and Western blotting, an equal volume of 4% paraformaldehyde or 1 ml ice-cold PBS, respectively, was added to stop the stimulation. For cytokine production assay, cells were incubated with complete medium containing PMA (2.5 ng/ml), ionomycin (1 μg/ml), and brefeldin A (1 μg/ml) at 37°C for 4 hours.

Immunoprecipitation and Western blot analysis. γδT cells were magnetically isolated from the thymus of 1-day-old mice using phycoerythrin-labeled (PE-labeled) anti-TCRδ (GL3) and anti-PE microbeads (Miltenyi Biotec). The purified γδT cells were stimulated with an anti-CD3ε antibody as described above. The cells were lysed with lysis buffer containing 50 mM Tris-HCl (pH7.5), 150 mM NaCl, 10 mM $MgCl_2$, 0.5% Nonidet P-40, 10% glycerol, and protease inhibitor cocktail (MilliporeSigma), as well as phosphatase inhibitor cocktail (Thermo Fisher Scientific). Cell lysates were incubated with anti-phosphotyrosine antibody (4G10) conjugated to Protein G Sepharose (GE Healthcare) at 4°C for 1 hour. Subsequently, the precipitates were washed and boiled in Laemmli gel-loading buffer. The proteins were subjected to SDS-PAGE and transferred onto a PVDF membrane.

IMQ-inducible psoriasis. For testing psoriasis-like dermatitis, a daily dose of 5 mg Beselna cream (5% IMQ; Mochida Pharmaceutical) or control vaseline cream (Wako) was applied to each ear for 6 days. Ear thickness was measured using a micrometer. On day 7, the ears were embedded in OCT compound (Sakura Finetek), sliced into 5-μm-thick sections with a Cryostat (Leica), air dried, fixed with acetone, and stained with H&E. The images were obtained with a Keyence BZ-9000 fluorescence microscope.

Statistics. All data are presented as the mean ± SEM. For statistical analysis, GraphPad Prism 6 (GraphPad Software) was used. A P value of less than 0.05 was considered statistically significant. A 2-tailed, unpaired t test was used for comparisons of 2 groups. A 1-way or 2-way ANOVA was used to compare 3 or more groups.

Study approval. All animal experiments were approved by the IRB of The University of Tokyo (approval I-H17-010) and the IACUC of the Research Institute of the National Center for Global Health and Medicine Research Institute (approvals 17024 and 17043) and were conducted in accordance with institutional protocols.

Author contributions

RM and TN performed most of the experiments, interpreted the results, and prepared the manuscript. KN and TO generated the genetically modified mice. HT provided advice on the project design and data interpretation and prepared the manuscript. HS supervised the project and wrote the manuscript.

Acknowledgments

We thank Robert E. Tigelaar (Yale University) for providing the 17D1 antibody and the late Leo Lefrançois (University of Connecticut Health Center) for providing the GL1 antibody. We thank S. Nitta, Y. Nakayama, M. Tsutsumi, T. Narita, T. Asano (The University of Tokyo), R. Yanobu-Takanashi, N. Tamehiro, and H. Oda (National Center for Global Health and Medicine) for technical assistance and all our laboratory members for helpful discussions. This study was supported by Grants-in-Aid for Research from the Japan Society for the Promotion of Science (JSPS) (KAKENHI 15H05703, 16H05202, and 16K19102); the National Center for Global Health and Medicine (grant 25-103, 26-105, 29-1001); and the Kanehara-Ichiro Foundation (grant 29–23).

Address correspondence to: Takeshi Nitta, Graduate School of Medicine and Faculty of Medicine, The University of Tokyo, 7-3-1, Hongo, Bunkyo-ku, Tokyo, 113-0033, Japan. Phone: 81.3.5841.3377; Email: nit-im@m.u-tokyo.ac.jp. Or to: Hiroshi Takayanagi, Graduate School of Medicine and Faculty of Medicine, The University of Tokyo, 7-3-1, Hongo, Bunkyo-ku, Tokyo, 113-0033, Japan. Phone: 81.3.5841.3373; Email: takayana@m.u-tokyo.ac.jp. Or to: Harumi Suzuki, Department of Immunology and Pathology, Research Institute, National Center for Global Health and Medicine, 1-7-1, Kounodai, Ichikawa-shi, Chiba, 272-8516, Japan. Phone:81.47.375.4764; Email: lbhsuzuki@hospk.ncgm.go.jp.

1. Shibata K. Close link between development and function of gamma-delta T cells. *Microbiol Immunol*. 2012;56(4):217–227.
2. Shichita T, et al. Pivotal role of cerebral interleukin-17-producing gammadeltaT cells in the delayed phase of ischemic brain injury. *Nat Med*. 2009;15(8):946–950.
3. Cai Y, et al. Pivotal role of dermal IL-17-producing γδ T cells in skin inflammation. *Immunity*. 2011;35(4):596–610.
4. Pantelyushin S, et al. Rorγt+ innate lymphocytes and γδ T cells initiate psoriasiform plaque formation in mice. *J Clin Invest*. 2012;122(6):2252–2256.
5. Wakita D, et al. Tumor-infiltrating IL-17-producing gammadelta T cells support the pro-

gression of tumor by promoting angiogenesis. *Eur J Immunol*. 2010;40(7):1927–1937.
6. Wu YL, et al. γδ T cells and their potential for immunotherapy. *Int J Biol Sci*. 2014;10(2):119–135.
7. Rei M, et al. Murine CD27(-) Vγ6(+) γδ T cells producing IL-17A promote ovarian cancer growth via mobilization of protumor small peritoneal macrophages. *Proc Natl Acad Sci U S A*. 2014;111(34):E3562–E3570.
8. Coffelt SB, et al. IL-17-producing γδ T cells and neutrophils conspire to promote breast cancer metastasis. *Nature*. 2015;522(7556):345–348.
9. Ono T, et al. IL-17-producing γδ T cells enhance bone regeneration. *Nat Commun*. 2016;7:10928.
10. Haas JD, et al. Development of interleukin-17-producing γδ T cells is restricted to a functional embryonic wave. *Immunity*. 2012;37(1):48–59.
11. Vantourout P, Hayday A. Six-of-the-best: unique contributions of γδ T cells to immunology. *Nat Rev Immunol*. 2013;13(2):88–100.
12. Jensen KD, et al. Thymic selection determines gammadelta T cell effector fate: antigen-naive cells make interleukin-17 and antigen-experienced cells make interferon gamma. *Immunity*. 2008;29(1):90–100.
13. Mahtani-Patching J, et al. PreTCR and TCRγδ signal initiation in thymocyte progenitors does not require domains implicated in receptor oligomerization. *Sci Signal*. 2011;4(182):ra47.
14. Prinz I, Silva-Santos B, Pennington DJ. Functional development of γδ T cells. *Eur J Immunol*. 2013;43(8):1988–1994.
15. Turchinovich G, Pennington DJ. T cell receptor signalling in γδ cell development: strength isn't everything. *Trends Immunol*. 2011;32(12):567–573.
16. Brownlie RJ, Zamoyska R. T cell receptor signalling networks: branched, diversified and bounded. *Nat Rev Immunol*. 2013;13(4):257–269.
17. Hayes SM, Love PE. Distinct structure and signaling potential of the gamma delta TCR complex. *Immunity*. 2002;16(6):827–838.
18. Dave VP, et al. CD3 delta deficiency arrests development of the alpha beta but not the gamma delta T cell lineage. *EMBO J*. 1997;16(6):1360–1370.
19. Blanco R, Borroto A, Schamel W, Pereira P, Alarcon B. Conformational changes in the T cell receptor differentially determine T cell subset development in mice. *Sci Signal*. 2014;7(354):ra115.
20. Muñoz-Ruiz M, et al. TCR signal strength controls thymic differentiation of discrete proinflammatory γδ T cell subsets. *Nat Immunol*. 2016;17(6):721–727.
21. van Oers NS, Lowin-Kropf B, Finlay D, Connolly K, Weiss A. alpha beta T cell development is abolished in mice lacking both Lck and Fyn protein tyrosine kinases. *Immunity*. 1996;5(5):429–436.
22. Page ST, van Oers NS, Perlmutter RM, Weiss A, Pullen AM. Differential contribution of Lck and Fyn protein tyrosine kinases to intraepithelial lymphocyte development. *Eur J Immunol*. 1997;27(2):554–562.
23. Laird RM, Laky K, Hayes SM. Unexpected role for the B cell-specific Src family kinase B lymphoid kinase in the development of IL-17-producing γδ T cells. *J Immunol*. 2010;185(11):6518–6527.
24. Mócsai A, Ruland J, Tybulewicz VL. The SYK tyrosine kinase: a crucial player in diverse biological functions. *Nat Rev Immunol*. 2010;10(6):387–402.
25. Negishi I, et al. Essential role for ZAP-70 in both positive and negative selection of thymocytes. *Nature*. 1995;376(6539):435–438.
26. Turner M, et al. Perinatal lethality and blocked B-cell development in mice lacking the tyrosine kinase Syk. *Nature*. 1995;378(6554):298–302.
27. Cheng AM, Rowley B, Pao W, Hayday A, Bolen JB, Pawson T. Syk tyrosine kinase required for mouse viability and B-cell development. *Nature*. 1995;378(6554):303–306.
28. Cheng AM, et al. The Syk and ZAP-70 SH2-containing tyrosine kinases are implicated in pre-T cell receptor signaling. *Proc Natl Acad Sci U S A*. 1997;94(18):9797–9801.
29. Rodriguez-Galán MC, Bream JH, Farr A, Young HA. Synergistic effect of IL-2, IL-12, and IL-18 on thymocyte apoptosis and Th1/Th2 cytokine expression. *J Immunol*. 2005;174(5):2796–2804.
30. Wencker M, et al. Innate-like T cells straddle innate and adaptive immunity by altering antigen-receptor responsiveness. *Nat Immunol*. 2014;15(1):80–87.
31. Okkenhaug K, Ali K, Vanhaesebroeck B. Antigen receptor signalling: a distinctive role for the p110delta isoform of PI3K. *Trends Immunol*. 2007;28(2):80–87.
32. Frauwirth KA, et al. The CD28 signaling pathway regulates glucose metabolism. *Immunity*. 2002;16(6):769–777.
33. Prinz I, Sansoni A, Kissenpfennig A, Ardouin L, Malissen M, Malissen B. Visualization of the earliest steps of gammadelta T cell development in the adult thymus. *Nat Immunol*. 2006;7(9):995–1003.
34. Palacios EH, Weiss A. Distinct roles for Syk and ZAP-70 during early thymocyte development. *J Exp Med*. 2007;204(7):1703–1715.
35. Mallick-Wood CA, et al. Disruption of epithelial gamma delta T cell repertoires by mutation of the Syk tyrosine kinase. *Proc Natl Acad Sci U S A*. 1996;93(18):9704–9709.
36. Gu Y, Chae HD, Siefring JE, Jasti AC, Hildeman DA, Williams DA. RhoH GTPase recruits and activates Zap70 required for T cell receptor signaling and thymocyte development. *Nat Immunol*. 2006;7(11):1182–1190.
37. Oda H, et al. RhoH plays critical roles in Fc epsilon RI-dependent signal transduction in mast cells. *J Immunol*. 2009;182(2):957–962.
38. Gray EE, et al. Deficiency in IL-17-committed Vγ4(+) γδ T cells in a spontaneous Sox13-mutant CD45.1(+) congenic mouse substrain provides protection from dermatitis. *Nat Immunol*. 2013;14(6):584–592.
39. Colucci F, et al. A new look at Syk in αβ and γδ T cell development using chimeric mice with a low competitive hematopoietic environment. *J Immunol*. 2000;164(10):5140–5145.
40. Chen Y, et al. Differential requirement of RasGRP1 for γδ T cell development and activation. *J Immunol*. 2012;189(1):61–71.
41. Zou W, Croke M, Fukunaga T, Broekelmann TJ, Mecham RP, Teitelbaum SL. Zap70 inhibits Syk-mediated osteoclast function. *J Cell Biochem*. 2013;114(8):1871–1878.
42. Latour S, Chow LM, Veillette A. Differential intrinsic enzymatic activity of Syk and Zap-70 protein-tyrosine kinases. *J Biol Chem*. 1996;271(37):22782–22790.
43. Grammatikos AP, Ghosh D, Devlin A, Kyttaris VC, Tsokos GC. Spleen tyrosine kinase (Syk) regulates systemic lupus erythematosus (SLE) T cell signaling. *PLoS One*. 2013;8(8):e74550.
44. Wang H, et al. ZAP-70: an essential kinase in T-cell signaling. *Cold Spring Harb Perspect Biol*. 2010;2(5):a002279.
45. Chu DH, Spits H, Peyron JF, Rowley RB, Bolen JB, Weiss A. The Syk protein tyrosine kinase can function independently of CD45 or Lck in T cell antigen receptor signaling. *EMBO J*. 1996;15(22):6251–6261.
46. Moon KD, et al. Molecular basis for a direct interaction between the Syk protein-tyrosine kinase and phosphoinositide 3-kinase. *J Biol Chem*. 2005;280(2):1543–1551.
47. Okada T, Maeda A, Iwamatsu A, Gotoh K, Kurosaki T. BCAP: the tyrosine kinase substrate that connects B cell receptor to phosphoinositide 3-kinase activation. *Immunity*. 2000;13(6):817–827.
48. Boomer JS, Green JM. An enigmatic tail of CD28 signaling. *Cold Spring Harb Perspect Biol*. 2010;2(8):a002436.
49. Kurebayashi Y, et al. PI3K-Akt-mTORC1-S6K1/2 axis controls Th17 differentiation by regulating Gfi1 expression and nuclear translocation of RORγ. *Cell Rep*. 2012;1(4):360–373.
50. Roller A, et al. Blockade of phosphatidylinositol 3-kinase PI3Kδ or PI3Kγ reduces IL-17 and ameliorates imiquimod-induced psoriasis-like dermatitis. *J Immunol*. 2012;189(9):4612–4620.
51. Shinkai Y, et al. Restoration of T cell development in RAG-2-deficient mice by functional TCR transgenes. *Science*. 1993;259(5096):822–825.
52. Mombaerts P, et al. Mutations in T-cell antigen receptor genes alpha and beta block thymocyte development at different stages. *Nature*. 1992;360(6401):225–231.
53. Itohara S, et al. T cell receptor delta gene mutant mice: independent generation of alpha beta T cells and programmed rearrangements of gamma delta TCR genes. *Cell*. 1993;72(3):337–348.
54. Roark CL, et al. Subset-specific, uniform activation among V gamma 6/V delta 1+ gamma delta T cells elicited by inflammation. *J Leukoc Biol*. 2004;75(1):68–75.
55. Goodman T, Lefrancois L. Intraepithelial lymphocytes. Anatomical site, not T cell receptor form, dictates phenotype and function. *J Exp Med*. 1989;170(5):1569–1581.
56. Nitta T, et al. The thymic cortical epithelium determines the TCR repertoire of IL-17-producing γδT cells. *EMBO Rep*. 2015;16(5):638–653.
57. Nitta T, Ohigashi I, Takahama Y. The development of T lymphocytes in fetal thymus organ culture. *Methods Mol Biol*. 2013;946:85–102.